MOLECULAR AND CELLULAR BIOLOGY, Jan. 1991, p. 38–46
0270-7306/91/010038-09$02.00/0

Vol. 11, No. 1

Intramitochondrial Functions Regulate Nonmitochondrial Citrate Synthase (*CIT2*) Expression in *Saccharomyces cerevisiae*

XINSHENG LIAO,[1] W. CURTIS SMALL,[1,2] PAUL A. SRERE,[1,2] AND RONALD A. BUTOW[1]*

Department of Biochemistry, University of Texas Southwestern Medical Center at Dallas, 5323 Harry Hines Boulevard, Dallas, Texas 75235,[1] and Veterans Administration Medical Center, Dallas, Texas 75216[2]

Received 23 July 1990/Accepted 18 September 1990

We have examined the effects of perturbation of mitochondrial function on expression of two nuclear genes encoding the mitochondrial and peroxisomal forms of citrate synthase in *Saccharomyces cerevisiae*, *CIT1* and *CIT2*. *CIT2* expression was as much as 30-fold higher in [*rho*^{0}] petites, than in isochromosomal [*rho*$^+$] cells, whereas *CIT1* expression was slightly down regulated in [*rho*^{0}] cells. *CIT2* expression was also increased in [*rho*$^+$] cells by inhibition of respiration with antimycin A or in [*rho*$^+$] cells containing a disruption of the *CIT1* gene. These effects were additive, and together they approached the level of *CIT2* expression seen in [*rho*^{0}] cells. Experiments using heterologous gene fusions showed that all of the effects leading to increased expression of *CIT2* were transcriptionally controlled through 5′-flanking *CIT2* DNA sequences. Analysis of [*rho*$^+$] and [*rho*^{0}] cells containing disruptions of *CIT1* and *CIT2*, singly and in combination, showed that the peroxisomal citrate synthase could partially spare the mitochondrial isoform for growth yield in [*rho*$^+$] but not in [*rho*^{0}] cells. These studies suggest a physiological role for increased expression of *CIT2* in cells with altered mitochondrial function. They also provide additional evidence for a retrograde path of communication from mitochondria to the nucleus in yeast cells.

It is well known that the nuclear genome plays a dominant role in determining mitochondrial structure and function and in providing most of the products that regulate the expression and maintenance of the mitochondrial genome (1, 37). Less clearly understood is how and to what extent such intramitochondrial events as the metabolic and respiratory state of the organelle or the quality and quantity of mitochondrial DNA affect the expression of nuclear genes. We previously hypothesized that such events could provide signals to the nucleus allowing the cell to monitor mitochondrial DNA content and mitochondrial mass or the general state of mitochondrial activity during cell growth and division (3). Recent studies have provided good evidence for such a retrograde path of communication from mitochondria to the nucleus (23–25, 38). It is also apparent that while the mitochondrial state can influence the expression of some nuclear genes encoding mitochondrial proteins, expression of other genes for nuclear-encoded mitochondrial proteins is unaffected (23, 24).

To explore further this complex interplay between mitochondria and the nucleus, we have investigated the effects of perturbations of mitochondrial function on the expression of two nuclear-encoded isoforms of citrate synthase in *Saccharomyces cerevisiae*: a mitochondrial form (CS 1) that is analogous to the protein found in mitochondria of higher eucaryotes and a nonmitochondrial form (CS 2) that is sequestered within peroxisomes (13, 17, 27, 29, 34). The nonmitochondrial isozyme is an activity that has been characterized only in *S. cerevisiae*.

CS 1 and CS 2 are highly homologous: 83% of their sequences either are identical or are conservative substitutions. The mitochondrial isoform is encoded by *CIT1*, and the peroxisomal isoform is encoded by *CIT2* (17, 29); these genes probably arose from the same ancestral gene by duplication followed by mutation (29). Although CS 1 and CS 2 are functionally equivalent activities, they participate in different metabolic cycles: CS 1 performs one of the integral functions of the tricarboxylic acid (TCA) cycle, while CS 2 probably participates in one or both of two nonmitochondrial metabolic pathways: the biosynthesis of glutamate, and the glyoxylate shunt used for growth on acetate or ethanol (16).

In this study, we analyzed the effects of alterations in mitochondrial function on *CIT1* and *CIT2* expression. We show that in [*rho*^{0}] petites, *CIT2* is transcriptionally activated as much as 30-fold compared with [*rho*$^+$] cells. We also present evidence that alteration of at least two distinct mitochondrial functions in [*rho*$^+$] cells transcriptionally activates *CIT2*. Finally, we present data to suggest that under certain conditions CS 2 activity may partly supplant CS 1 activity for cell growth and growth yield.

MATERIALS AND METHODS

Chemicals. Triton X-100, D,L-isocitrate, oxaloacetate, coenzyme A, glucose, raffinose, ethidium bromide, sorbitol, mannitol, and NAD$^+$ were from Sigma (St. Louis, Mo.). Acetyl coenzyme A was prepared by the treatment of coenzyme A with acetic anhydride as described previously (32).

Strains and growth conditions. Ten strains of *S. cerevisiae* with different nuclear and mitochondrial genotypes were used. They include five [*rho*$^+$] strains with different nuclear genotypes and their corresponding [*rho*^{0}] derivatives: PSY142 (*MAT*α *leu2-2 leu2-112 lys 2-801 ura 3-52*); PSY142 CS1$^-$ (*MAT*α *leu2-2 leu2-112 lys2-801 ura3-52 cit1::LEU2*), PSY142 CS2$^-$ (*MAT*α *leu2-2 leu2-112 lys2-801 ura3-52 cit2::URA3*), PSY142 CS1$^-$ CS2$^-$ (*MAT*α *leu2-2 leu2-112 lys2-801 ura3-52 cit1::LEU2 cit2::URA3*), and COP161 U7 (*MAT***a** *ade lys ura3*). Cells were grown on YP medium (1% yeast extract, 2% Bacto-Peptone [Difco Laboratories]) with either 5% glucose (YPD) or 2% raffinose (YPR) as the carbon source. The [*rho*^{0}] derivatives of the strains used were

* Corresponding author.

obtained by growing cells for ~40 generations in YPD medium containing 20 μg of ethidium bromide per ml. Isolates were verified as [*rho*^{0}] by 4,6-diamidino-2-phenylindole staining. In most cases, cells were grown as 50-ml (for isolation of RNA) or 750-ml (for enzyme activity assay) cultures in either YPR or YPD as specified in the text and harvested at between 0.2 and 1.0 A_{600} units. Cell growth was determined turbidometrically. Yeast transformations were carried out by the lithium acetate procedure as described by Ito et al. (12).

Plasmids. pCS106 is a pBR322-based plasmid containing 1.4 kb of the *CIT2* coding region plus 1 kb of 5′- and 3′-flanking DNA on a 3.4-kb *Eco*RI fragment (29). pFCS1 contains the *CIT1* gene on a 4.5-kb *Bam*HI fragment (34). pSEY101 is a 2 μm-based shuttle vector containing the *Escherichia coli lacZ* gene (6). pRS315 is an *ARS-CEN* shuttle vector containing the *LEU2* gene (31). pBL101 is an *ARS-CEN* plasmid containing the *URA3* gene and 5′ *CYC1* sequences fused in frame to the *E. coli lacZ* gene. pYact-1 contains the actin gene on a 3.8-kb *Eco*RI fragment (20).

Construction of plasmids and fusion genes. p*CIT2*-605-LacZ contains a 605-bp *Hin*fI fragment of the 5′ region of *CIT2* fused in frame to the *E. coli lacZ* gene. This *CIT2* sequence includes 530 bp of the 5′ region of *CIT2* plus sequences encoding the first 24 amino acids fused in frame to *lacZ*. To construct p*CIT2*-605-LacZ, *Bam*HI linkers were added to the 605-bp *Hin*fI *CIT2* fragment from pCS106, and the fragment was ligated into the *Bam*HI site of pSEY101. Subsequently, a 2.5-kb *Sma*I-*Sst*I fragment containing the 605-bp 5′ *CIT2* sequences plus *lacZ* DNA from pSEY101 was inserted into the *Sma*I-*Sst*I sites of pBL101. pRS-*CIT2* contains a 3.4-kb *Eco*RI *CIT2* fragment from pCS106, which was constructed by ligating the 3.4-kb *Eco*RI fragment, following fill-in with the Klenow fragment of DNA polymerase I, into the *Sma*I site of pRS315. pRSAct-*CIT2* is a fusion between the actin gene promoter region and the *CIT2* coding region (plus 3′-flanking DNA sequences). A 464-bp *Alu*I fragment of 5′ actin sequences from pYact-1 was inserted into the *Sma*I site of pRS315. An *Spe*I-*Xba*I fragment downstream of the actin insert was removed and replaced with an *Spe*I-*Eco*RI fragment of *CIT2* from pCS106.

RNA isolation. Total cellular RNA was extracted from exponentially growing yeast cells by the method of Elion and Warner (7) except that the lysis buffer contained 50 mM Tris hydrochloride (pH 8.0), 0.1 M NaCl, 50 mM sodium acetate, 10 mM EDTA, and 0.5% sodium dodecyl sulfate. The RNA prepared in this way was digested with RNase-free DNase and stored in 70% ethanol at −20°C.

RNase protection analysis. RNase protection experiments were carried out essentially as described by Melton et al. (19). All probes used in the RNase protection study were antisense RNA probes synthesized in vitro, by either SP6 or T7 RNA polymerase, as described previously (19). The probe to actin was prepared as previously described (23) except that the plasmid was linearized with *Bgl*II. The actin probe is 323 nucleotides (nt) long, and the protected one is 282 nt long. For the *CIT1* probe, a 471-bp *Bgl*II-*Eco*RI fragment of *CIT1* internal to the coding region was subcloned from pFCS1 into the *Bam*HI-*Eco*RI sites of pGEM 3Zf(+). The *CIT1* RNA probe was generated by using T7 RNA polymerase, and the plasmid was linearized by digestion with *Hin*dIII. The length of *CIT1* probe is 502 nt long, and the protected one is 471 nt long. Two *CIT2* probes were used. For most of the experiments measuring *CIT2* mRNA levels, a 1,083-bp *Spe*I-*Nco*I *CIT2* fragment was subcloned into the corresponding sites in pGEM 5Zf(+). The plasmid was linearized with *Ava*II and transcribed by T7 RNA polymerase to yield a full-length 444-nt probe; the size of the protected fragment is 407 nt. The *CIT2* riboprobe used for Fig. 3 and 6 was generated by subcloning a 1-kb *CIT2* *Pvu*II-*Stu*I fragment into the *Sma*I site of pGEM 3Zf(+). The plasmid was linearized with *Sca*I and transcribed with SP6 RNA polymerase, yielding a full-length 800-nt probe containing internal *CIT2* coding sequences and sequences from the 3′ nontranscribed region. The specific activity of each probe was adjusted by the concentration (100 to 500 μM) of cold UTP added in the reaction mixture. The amount of total cellular RNA used in the experiments ranged from 10 to 60 μg, and the amount of probe varied from 4×10^4 to 10^5 cpm. Autoradiograms were quantified by scanning with a Molecular Dynamics densitometer.

S1 nuclease protection analysis. A 734-bp *CIT2* DNA fragment from an upstream *Dde*I site to a *Bst*NI site within the *CIT2* coding region was isolated, treated with calf intestine alkaline phosphatase, and end labeled with ^{32}P by T4 polynucleotide kinase. S1 nuclease protection analysis was carried out with total cellular RNA as described by Zhu et al. (40) except that the hybridization temperature was at 37 instead of 42°C. S1-protected fragments were mapped to *CIT2* sequences by comparison with a sequencing ladder generated by dideoxy sequencing of the 605-bp *CIT2* *Hin*fI fragment, described above, cloned into M13mp19.

Subcellular fractionation and quantitation of enzymatic activities. Mitochondria were isolated by the method of Daum et al. (5) as described by Rosenkrantz et al. (29). The supernatant fraction from the centrifugation which produced the mitochondrial pellet was assumed to be the cytosol and was used without further treatment. Citrate synthase assays were conducted by the spectrophotometric method of Srere et al. (33). Mitochondria for these determinations were dissolved in a buffer containing 50 mM Tris hydrochloride (pH 8.1), 1 mM disodium EDTA, and 0.2% Triton X-100 at least 60 min before initiation of the assay. CS 2 is known to be unstable at this pH (29), and >90% of any residual CS 2 activity in the mitochondrial preparation is inactivated by this procedure (unpublished data). To measure expression of β-galactosidase, 10 independent p*CIT2*-605-LacZ transformants of the various cell types (see Results) were pooled and grown on YPR, and β-galactosidase activity was measured in cell extracts as described previously (28). In some cases, we detected significant loss (>50% of the cells) of plasmid p*CIT2*-605-LacZ from cells grown on rich (YP) medium. Thus, all β-galactosidase activities have been corrected for plasmid content as determined by replica plating to selective and nonselective media. Protein concentrations were estimated by the method of Bradford (2), using bovine serum albumin as a standard.

Nucleotide sequence accession number. The sequence reported has been assigned GenBank accession number M54982.

RESULTS

***CIT1* and *CIT2* are differentially regulated in [*rho*$^+$] and [*rho*^{0}] cells.** Enzyme assays specific for CS 1 and CS 2 activities were carried out on mitochondrial and supernatant fractions to determine the amount of these activities in [*rho*$^+$] and [*rho*^{0}] derivatives of two yeast strains, COP161 U7 and PSY142 (Table 1). These strains were grown on 5% glucose (YPD) and on 2% raffinose (YPR), a nonrepressing carbon source. In agreement with previous findings (21), CS 1 activity was glucose repressible, as are most enzymes of

TABLE 1. CS 1 and CS 2 activities in [*rho*$^+$] and [*rho*^{0}] strains grown on glucose and on raffinose[a]

Enzyme	Strain	Carbon source	Activity (nmol/min/mg)
CS 1	COP161 U7 [*rho*$^+$]	Glucose	127.1 ± 46.0 (12)[b]
		Raffinose	866.1 ± 64.5 (4)
	COP161 U7 [*rho*^{0}]	Glucose	78.0 ± 46.9 (14)
		Raffinose	222.8 ± 79.0 (7)
	PSY142 [*rho*$^+$]	Glucose	347.3 ± 48.3 (3)
		Raffinose	581.4 ± 84.6 (2)
	PSY142 [*rho*^{0}]	Glucose	25.2 ± 7.8 (5)
		Raffinose	138.5 ± 8.2 (2)
	PSY142 [*rho*$^+$] CS1$^-$	Glucose	0.3 ± 0.1[c] (2)*
		Raffinose	0.1 ± 0.1[c] (2)
	PSY142 [*rho*^{0}] CS1$^-$	Glucose	0.4 ± 0.1[c] (2)
		Raffinose	0.6 ± 0.2[c] (2)
CS 2	COP161 U7 [*rho*$^+$]	Glucose	8.3 ± 7.3 (19)
		Raffinose	18.4 ± 1.3 (4)
	COP161 U7 [*rho*^{0}]	Glucose	12.6 ± 9.6 (9)
		Raffinose	202.9 ± 73.2 (3)
	PSY142 [*rho*$^+$]	Glucose	13.1 ± 1.1 (2)
		Raffinose	45.5 ± 13.7 (4)
	PSY142 [*rho*^{0}]	Glucose	11.3 ± 1.5 (2)
		Raffinose	372.0 ± 42.7 (2)
	PSY142 [*rho*$^+$] CS1$^-$	Raffinose	292.6 ± 40.5 (4)
	PSY142 [*rho*^{0}] CS1$^-$	Raffinose	156.3 ± 19.3 (4)

[a] CS 1 and CS 2 enzyme assays were carried out as described in Materials and Methods. The PSY142 CS1$^-$ cells contain a *URA3* disruption of *CIT1*. Strains were grown in YP medium containing 5% glucose or 2% raffinose as indicated.

[b] Number in parentheses is number of experiments.

[c] Residual CS 2 activity.

the TCA cycle. CS 1 activity in both glucose- and raffinose-grown cells was 1.6- to 13.8-fold lower in the [*rho*^{0}] petite derivatives than in the [*rho*$^+$] parents; as expected, we detected little or no CS 1 activity in PSY142 cells harboring a *CIT1* deletion (Table 1).

In [*rho*$^+$] cells, CS 2 activity was modestly reduced by growth on glucose (Table 1). In [*rho*^{0}] cells, CS 2 activity, in contrast to CS 1 activity, was 8- to 11-fold greater than in the [*rho*$^+$] strains when these cells were grown on raffinose; however, there was no such induction of CS 2 activity in either COP161 U7 or PSY142 when these strains were grown on glucose. Finally, [*rho*$^+$] PSY142 cells with a *CIT1* disruption (which therefore lack CS 1 activity) contained more than six times the amount of CS 2 activity found in wild-type [*rho*$^+$] cells.

To correlate these enzyme activity data with mRNA levels, we used an RNase protection assay with riboprobes both complementary and internal to *CIT1*, *CIT2*, and actin mRNAs. Actin mRNA serves as a suitable internal control for RNA input in these experiments, since that message abundance is unaffected either by the carbon source or by the respiratory state of the cell (24, 35). To validate this assay, we compared the signal obtained for the RNase-protected *CIT1* fragment at three different RNA inputs, using total RNA isolated from COP161 U7 [*rho*$^+$] and [*rho*^{0}] cells grown in YPD medium. The observed signal was proportional to RNA input, and the [*rho*^{0}] cells contained slightly less *CIT1* mRNA than did the [*rho*$^+$] cells (Fig. 1A). Data obtained from a direct comparison of *CIT1* mRNA abundance in [*rho*$^+$] and [*rho*^{0}] cells grown in YPD or YPR medium (Fig. 1B) were in qualitative agreement with the enzyme data of Table 1: *CIT1* expression was glucose repressible and generally lower in [*rho*^{0}] than in [*rho*$^+$] cells.

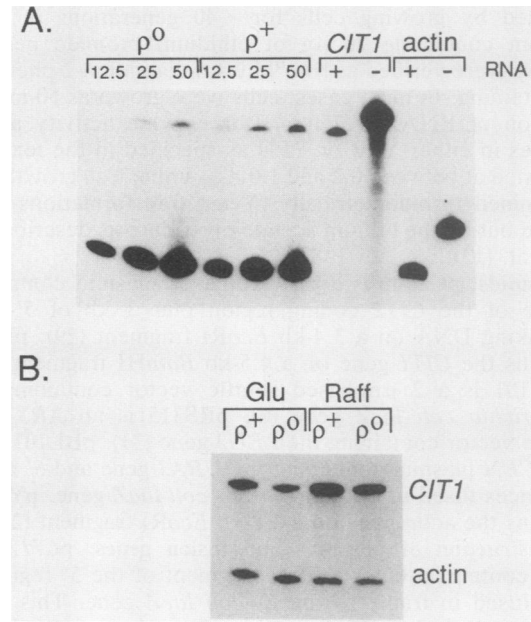

FIG. 1. RNase protection analysis of steady-state *CIT1* mRNA levels. (A) ^{32}P-labeled antisense RNA probes internal to *CIT1* and actin mRNAs described in Materials and Methods were hybridized with or without the indicated amounts (in micrograms) of total cellular RNA prepared from COP161 U7 [*rho*$^+$] and [*rho*^{0}] cells growing exponentially in YPD medium. Unhybridized probes were digested with RNases A and T_1 (see Materials and Methods). The −RNA lanes represent undigested intact probe. All fragments were resolved on a 5% polyacrylamide–8 M urea gel. The protected *CIT1* probe is 471 nt long, and the protected actin probe is 282 nt long. The lengths of the intact *CIT1* and actin probes are 502 and 323 nt, respectively. (B) RNase protection analysis of *CIT1* mRNA levels in COP161 U7 [*rho*$^+$] and [*rho*^{0}] cells growing exponentially on YPD (Glu) or YPR (Raff) medium.

RNase protection experiments with the *CIT2*-specific probe hybridized to total RNA from COP161 U7 cells grown on raffinose showed a significantly greater level of *CIT2* mRNA in the [*rho*^{0}] petite cells than in [*rho*$^+$] cells, also in agreement with the enzyme activity data of Table 1 (Fig. 2). (The doublet seen for the *CIT2*-protected fragment in these and subsequent experiments may be the result of some

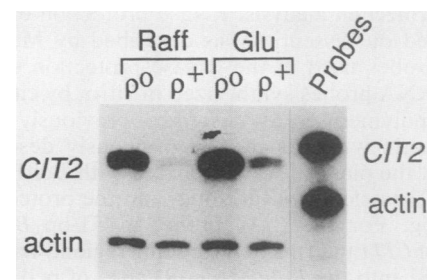

FIG. 2. RNase protection analysis of steady-state levels of *CIT2* mRNA in COP161 U7 [*rho*$^+$] and [*rho*^{0}] cells. Total cellular RNA was isolated from exponentially growing cultures of COP161 U7 [*rho*$^+$] and [*rho*^{0}] cells grown in YPR (Raff) or YPD (Glu) medium and used in RNase protection assays to determine the level of *CIT2* mRNA as described in the legend to Fig. 1 and in Materials and Methods. The length of the intact *CIT2* probe complementary to *CIT2* mRNA is 444 nt; the length of the protected probe is 407 nt.

"breathing" between the *CIT2* riboprobe and *CIT2* message: by Northern [RNA] blot analysis, we observed only a single *CIT2* RNA species when we used the same complementary riboprobe [data not shown].) In 16 independent experiments with cells grown on raffinose, the *CIT2* mRNA level was 6- to 15-fold greater in [*rho*^{0}] than in [*rho*$^+$] cells, and the average specific activity of CS 2 in [*rho*^{0}] cells was 11-fold greater than in [*rho*$^+$] cells.

In cells grown on glucose, the steady state-level of *CIT2* mRNA showed two patterns. In the experiment shown in Fig. 2, the [*rho*^{0}] cells appeared to contain higher levels of *CIT2* mRNA than did the [*rho*$^+$] cells, but in other experiments there was little or no difference in *CIT2* mRNA abundance between [*rho*$^+$] and [*rho*^{0}] cells. In more than 10 independent experiments in which *CIT2* mRNA levels were measured in cells grown on glucose, the results were divided about equally between these two findings. However, in no experiment did we detect any significant difference between [*rho*$^+$] and [*rho*^{0}] cells in CS 2 enzyme activity (Table 1). We have no explanation for this variability in *CIT2* mRNA levels between [*rho*$^+$] and [*rho*^{0}] cells grown on glucose, though we do know that it cannot be explained simply by derepression of cells, since glucose is exhausted from the medium (data not shown). In all subsequent experiments presented here, cells were grown in YPR medium.

Transcription of *CIT2* initiates at −61 bp upstream of the ATG in [*rho*$^+$] and [*rho*^{0}] cells. To map the 5′ end(s) of the *CIT2* mRNA and to determine whether there are differences between [*rho*$^+$] and [*rho*^{0}] cells, we carried out S1 nuclease protection experiments by using a 734-bp probe hybridized to total RNA from [*rho*$^+$] and [*rho*^{0}] cells (Fig. 3). Although the signal for S1-protected fragments was much greater in [*rho*^{0}] than in [*rho*$^+$] cells, as expected from the findings presented above, there was no difference in the size of the protected fragments. The largest S1-protected fragment maps to position −61 from the ATG start (Fig. 4). That putative transcriptional start site is 75 bp downstream of a candidate TATA box at position −135.

CS 2 partially spares CS 1 for growth yield in [*rho*$^+$] but not in [*rho*^{0}] cells. One explanation previously advanced to account for the elevated expression of some nuclear genes in respiratory-deficient cells is that increases in expression represent attempts, though perhaps futile in petites, to compensate for the respiratory-deficient state (3). To investigate the physiological significance of the elevated *CIT2* expression in a [*rho*^{0}] petite, we compared growth rates and growth yields in YPR medium of wild-type [*rho*$^+$] and [*rho*^{0}] PSY142 strains and their derivatives containing single or double disruptions of *CIT1* and *CIT2*. Neither the single disruptions nor the double disruption had any significant effect on growth yield in the [*rho*^{0}] cells; growth rate was also unaffected except for a slight (7%) reduction in the double-deletion strain (Table 2). In [*rho*$^+$] cells, a disruption of *CIT1* significantly lowered the growth yield, as would be expected for a block in the TCA cycle, while disruption of *CIT2* had no effect on either growth rate or growth yield in [*rho*$^+$] or [*rho*^{0}] cells. However, in the double-deletion [*rho*$^+$] strain lacking both CS 1 and CS 2 activities, the growth rate was reduced to about 75% of the wild-type rate and the growth yield was reduced to nearly one-half. These results suggest that in the [*rho*$^+$] cells, CS 2 activity can partially compensate for the absence of CS 1 activity. In the [*rho*^{0}] cells, the absence of any respiratory function apparently obscures the effects on growth yield when CS 1 and CS 2 activities are lacking.

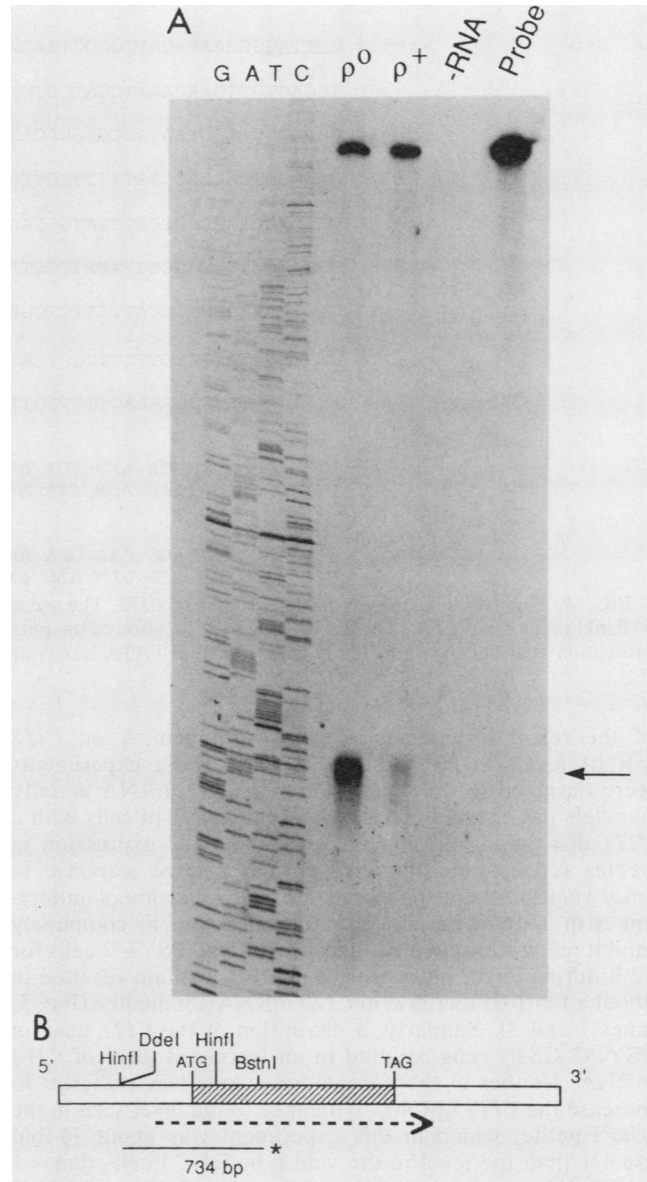

FIG. 3. (A) S1 nuclease mapping of the 5′ ends of the *CIT2* mRNA in [*rho*$^+$] and [*rho*^{0}] cells. A 734-bp DNA fragment of *CIT2* from a *Dde*I-to-*Bst*NI site was end labeled with ^{32}P by T4 polynucleotide kinase, denatured, and hybridized with total cellular RNA from COP161 U7 [*rho*$^+$] and [*rho*^{0}] cells growing on YPR medium as described in Materials and Methods. The hybridization and S1 nuclease digestion conditions were the same as described by Zhu et al. (40) except that hybridization was carried out at 37°C. Since ends of the fragment are 5′ overhangs, no labeled intact probe is detected. The sequence ladder (lanes G, A, T, and C) was generated from a single-stranded M13 clone containing a 605-bp *Hin*fI fragment of 5′ *CIT2* sequences shown in panel B. That *Hin*fI fragment containing *Bam*HI linkers was cloned into the *Bam*HI site of M13mp19 and sequenced by dideoxy-chain termination (30). The largest S1-protected fragment corresponds to a 5′ end at position −61 from the ATG start codon as indicated in Fig. 4. The dotted line indicates the *CIT2* transcript.

***CIT2* expression is increased in [*rho*$^+$] cells by the addition of a respiratory inhibitor and by a disruption of *CIT1*.** The enzyme activity data in Table 1 show that in [*rho*$^+$] cells, a *CIT1* disruption resulted in elevated CS 2 activity. We next examined the effects of the *CIT1* disruption and the addition

```
                                                                -533 AAT
-530 CCTTAGGGGAAAACATTGCGCTGACTTTCCCCAGAGTTGTTGCCACAACATAAGCCGCTT
       DdeI
-470 TGGAGTGTTGAACAAATCCGTCCTTGGGTCATTCAATCAATGGCTTGGCGGTATCTCAAA

-410 AGAGCGCAAACTAATAGCGCGCACATTCGACGCATTTATCCGGTGGTCATCGACAGGGGC
                                          MspI
-350 GAAAGGTCACGACCTATTTTTTCTTGCAGAAAAAAAGTGTGACCTTTTCCGTAGCTAGAC
                                                          AluI
-290 GTCTATCAGGGCGTCAGCAATGGGAGGCACAGCGGAAAAACAATAACAATGGTAAGCGCA

-230 ATTACCTTTTGAGCGTTACATTCGTATGAAATTGGTGACGTTAATCTAAAGATAGTCATG

-170 CTCTCAAAAGGGCCCATTATTCTCGACGTTGAGCGTATATAAGACTATTAAAACTTGGTT

-110 CTTTAGATATGGTGTTCGTTCCTCATTATTAAGTTTCAGGGAACAATATCAACACATATC
                                                              +1
-50  ATAACAGGTTCTCAAAACTTTTTGTTTTAATAATACTAGTAACAAGAAAA ATG ACA
                                          SpeI                MET THR

     GTT CCT TAT CTA AAT TCA AAC AGA AAT GTT GCA TCA TAT TTA CAA
     VAL PRO TYR LEU ASN SER ASN ARG ASN VAL ALA SER TYR LEU GLN


     TCA AAT TCA AGC CAA GAA AAG
     SER ASN SER SER GLN GLU LYS
```

FIG. 4. Nucleotide sequence of the 5′ region of *CIT2*. The sequence presented extends the available published sequence data (29) for the 5′-flanking region of *CIT2*. The arrow shows the location of the putative most 5′ transcriptional start site, as determined from the S1 nuclease protection analysis shown in Fig. 4. The probable TATA box is underscored with a double line. Relevant restriction sites are indicated.

of the respiratory chain inhibitor antimycin A on *CIT2* mRNA levels in PSY142 [*rho*$^+$] cells. These experiments were designed to determine whether *CIT2* mRNA activity parallels the enzyme activity data of Table 1 in cells with a *CIT1* disruption and whether elevated *CIT2* expression in petites reflects an otherwise normal control response in [*rho*$^+$] cells to the respiratory state. The inclusion of antimycin A at 1 μg/ml (a concentration sufficient to completely inhibit respiration) to a culture of wild-type PSY142 cells for 12 h during logarithmic growth in YPR medium resulted in about a fourfold increase in *CIT2* mRNA abundance (Fig. 5, lanes 1 and 3). Similarly, a disruption of the *CIT1* gene in PSY142 CS1$^-$ cells resulted in an increased level of *CIT2* mRNA. Neither of these conditions alone was sufficient to increase the *CIT2* mRNA abundance to the level seen in the [*rho*^{0}] petite, which in this experiment was about 30-fold greater than the level in the wild-type [*rho*$^+$] cells (lanes 1 and 2). However, the addition of antimycin A to PSY142 CS1$^-$ [*rho*$^+$] cells (lane 5) resulted in an increase of *CIT2* mRNA, comparable to the RNA abundance in [*rho*^{0}] cells (compare lanes 2 and 5). Thus, disruption of the *CIT1* gene and inhibition of mitochondrial respiration appear to be additive in signaling an elevated expression of *CIT2* mRNA.

Increased *CIT2* expression in cells with perturbed mitochondrial function is transcriptional and depends on 5′-flanking *CIT2* DNA sequences. To define further the effect of perturbation of mitochondrial function on *CIT2* expression, we analyzed two heterologous gene constructs of *CIT2* placed in *ARS-CEN* plasmids to determine whether the differences in expression are due to transcriptional or posttranscriptional events. In one construct, pRAct-*CIT2*, a 464-bp fragment consisting of the yeast actin promoter (20), was fused to the coding and 3′-flanking regions of the *CIT2* gene (Fig. 6A). That construct and one (pRS-*CIT2*) containing the entire *CIT2* gene, used as a control (Fig. 6A), were transformed into PSY142 cells in which the *CIT2* gene had been disrupted by *URA3* (Fig. 6B). Using an 800-nt riboprobe that spans the

TABLE 2. Comparison of growth rate and growth yield in [*rho*$^+$] and [*rho*^{0}] PSY142 cells with single and double disruptions of *CIT1* and *CIT2*[a]

PSY142 nuclear genotype	[*rho*^{0}]		[*rho*$^+$]	
	Doubling time (h)	Growth yield[b]	Doubling time (h)	Growth yield
CIT1 CIT2	3.86	136	2.20	452
cit2::*URA3*	3.84	138	2.21	433
cit1::*LEU2*	3.66	121	2.38	340
cit2::*URA3* *cit1*::*LEU2*	4.13	139	2.86	250

[a] Cells were grown in YPR medium as described in Materials and Methods. Cell growth and growth yields were determined turbidometrically.
[b] Klett values (no. 66 filter) obtained for maximal cell density.

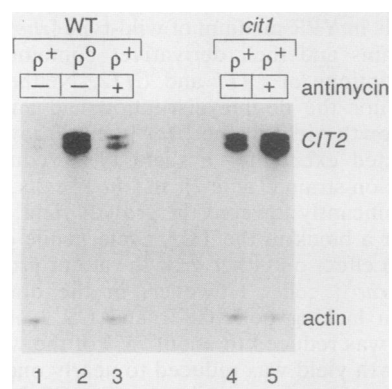

FIG. 5. Additive induction of *CIT2* mRNA in [*rho*$^+$] cells by antimycin A and by a disruption of the *CIT1* gene. PSY142 wild-type [*rho*$^+$] and [*rho*^{0}] and PSY142 CS1$^-$ (*cit1*) cells were grown for 12 h in YPR medium in the presence (+) or absence (−) of antimycin (1 μg/ml). *CIT2* mRNA levels were measured by RNase protection as described in the legend to Fig. 1 and in Materials and Methods.

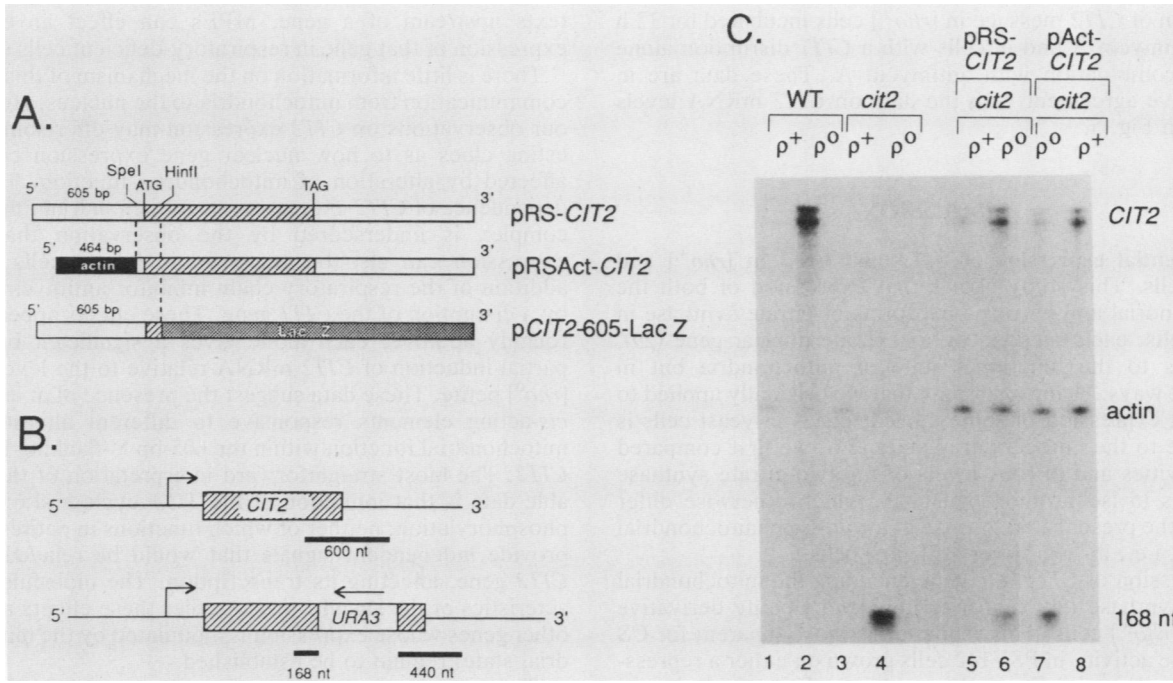

FIG. 6. Regulation of *CIT2* expression by 5'-flanking sequences. (A) Constructs used. See Materials and Methods for details. pRS-*CIT2* contains the wild-type *CIT2* gene; pRSAct-*CIT2* contains 464 bp of the 5' actin gene fused into the *Spe*I site of *CIT2*; p*CIT2*-605-LacZ contains a 605-bp *Hin*fI fragment of *CIT2* that includes a portion of the coding sequences fused in frame to the *E. coli lacZ* gene. These constructs were transformed into PSY142 wild-type or PSY142 CS2$^-$ (*cit2*) strains as indicated in panel C and in Table 3. (B) Diagram of RNase protection of transcripts from the wild-type *CIT2* gene, which would yield a ~600-nt protected fragment (see Materials and Methods), either endogenous or in pRS-*CIT2*, and two predicted RNase-protected fragments of 168 and 440 nt from PSY142 CS2$^-$. (C) RNase protection analysis of PSY142 wild-type and PSY142 CS2$^-$ (*cit2*) [*rho*$^+$] and [*rho*^{0}] strains. Lanes: 1 and 2, PSY142 nontransformed; 3 and 4, PSY142 CS2$^-$; 5 and 6, PSY142 *cit2*::*URA3* transformed with pRS-*CIT2*; 7 and 8, PSY142 CS2$^-$ transformed with pAct-*CIT2*. The predicted 440-nt protected fragment from the *cit2*::*URA3* locus is not evident, probably because *CIT2* transcription does not efficiently extend past *URA3* (see text).

CIT2 coding and 3' nontranslated regions, and thus crosses the *URA3* disruption of the endogenous *CIT2* gene (Fig. 6B), we could distinguish transcripts of the endogenous gene from those of pRS-*CIT2* and pRSAct-*CIT2*: transcripts from the endogenous gene yielded RNase-protected fragments of 168 and 440 nt, while transcripts from pRS-*CIT2* or pRS-ACT-*CIT2* yielded a fully protected 600-nt fragment (Fig. 6C). In the control experiments (lanes 1 to 4), the 168-nt protected fragment corresponding to transcripts from the disrupted *CIT2* gene was elevated to the same extent in a [*rho*^{0}] petite as were the transcripts from the wild-type endogenous gene, which in this experiment were ~30-fold greater in the [*rho*^{0}] than in the [*rho*$^+$] cells (compare lanes 3 and 4 with lanes 1 and 2). Similarly, transcripts derived from cells harboring the intact *CIT2* gene on pRS-*CIT2* were five- to sixfold higher in [*rho*^{0}] than in [*rho*$^+$] cells (lanes 5 and 6). However, when the *CIT2* promoter was replaced by the actin promoter in pRSAct-*CIT2*, there was no increase in transcript abundance of *CIT2* sequences in [*rho*^{0}] cells, indicating that 5'-flanking *CIT2* sequences are required for the [*rho*^{0}]-dependent increase in RNA. In these experiments, we did not observe the predicted 440-nt protected fragment (Fig. 6B). A plausible explanation for the failure to see this species is that transcription of *CIT2* does not efficiently extend past the 3' end of *URA3*, which is transcribed in the direction opposite that of *CIT2*.

These results indicate that the increase in *CIT2* expression in [*rho*^{0}] petite cells is conferred transcriptionally through its 5'-flanking DNA sequences. To confirm this conclusion, and to determine whether the same 5' sequences are also required for increased *CIT2* expression by inhibition of respiration or by loss of CS1$^-$ activity, we examined β-galactosidase activity in cells transformed with a plasmid containing a *CIT2-lacZ* fusion. For these experiments, 605 bp of the 5'-flanking region of *CIT2*, including the first 24 codons of the *CIT2* reading frame (Fig. 4 and 6), were fused in frame to the *E. coli lacZ* gene. The resultant construct, p*CIT2*-605-LacZ (Fig. 6A), was transformed into [*rho*$^+$] and [*rho*^{0}] cells. This fusion gene transformed into [*rho*^{0}] cells expressed over eightfold more β-galactosidase activity than did [*rho*$^+$] transformants (Table 3). This result is consistent with the findings discussed above indicating that the 5' region of *CIT2* is sufficient to account for the enhanced expression of *CIT2* in [*rho*^{0}] petites. Those same 5' sequences also account for the

TABLE 3. Effects of perturbation of mitochondrial function on β-galactosidase activity in cells transformed with p*CIT2*-605-LacZ[a]

Strain	Addition	β-Galactosidase activity[b] (nmol/min/mg)
PSY142 [*rho*$^+$]	None	378 ± 3
PSY142 [*rho*$^+$]	Antimycin A (1 μg/ml)	788 ± 16
PSY142 [*rho*$^+$] CS1$^-$	None	2,145 ± 22
PSY142 [*rho*$^+$] CS1$^-$	Antimycin A (1 μg/ml)	2,632 ± 84
PSY142 [*rho*^{0}]	None	3,100 ± 33

[a] PSY142 [*rho*$^+$] cells and its derivatives as indicated were transformed with p*CIT2*-605-LacZ and grown in YPR medium.
[b] Measured in cell extracts as described in Materials and Methods.

induction of *CIT2* message in [*rho*$^+$] cells incubated for 12 h with antimycin A and in cells with a *CIT1* disruption alone and in combination with antimycin A. These data are in qualitative agreement with the data on *CIT2* mRNA levels shown in Fig. 5.

DISCUSSION

Differential expression of *CIT1* and *CIT2* in [*rho*$^+$] and [*rho*^{0}] cells. This study shows that expression of both the mitochondrial and peroxisomal forms of citrate synthase in yeast cells, each encoded by a separate nuclear gene (29), responds to the functional state of mitochondria but in different ways. Using a strategy that we originally applied to find that expression of some nuclear genes in yeast cells is sensitive to the mitochondrial state (24), we first compared the activities and mRNA levels of the two citrate synthase isozymes in isochromosomal cells, which otherwise differ only by the presence or absence of a wild-type mitochondrial genome, i.e., in [*rho*$^+$] versus [*rho*^{0}] cells.

Expression of *CIT1*, the gene encoding the mitochondrial citrate synthase (29), is lower in a [*rho*^{0}] petite derivative than in [*rho*$^+$] cells. This reduction is most apparent for CS 1 enzyme activity in PSY142 cells grown on either a repressing or a derepressing carbon source. This result is not surprising for the expression of a nuclear gene encoding a mitochondrial protein whose activity would not be required in respiratory-deficient cells. However, the expression of other nuclear-encoded mitochondrial proteins, which also have no obvious function in respiratory-deficient cells, is unaffected in petites (4, 8, 24).

In contrast to the results for *CIT1*, both enzyme and mRNA products of *CIT2*, which encodes the peroxisomal form of citrate synthase (17, 29), are dramatically and reproducibly elevated in [*rho*^{0}] petites compared with [*rho*$^+$] cells when those cells are grown on raffinose. Although we have not detected any significant differences in CS 2 enzyme activity between [*rho*$^+$] and [*rho*^{0}] cells grown on glucose, we have observed in some experiments an increase in *CIT2* mRNA abundance, comparable to that seen for raffinose-grown cells. However, for unknown reasons, this effect is variable. The results of S1 nuclease protection experiments indicate that the same transcriptional start site is used in [*rho*^{0}] and [*rho*$^+$] cells, at position −61 from the translational start of *CIT2*.

Increased *CIT2* expression by alteration of mitochondrial function is transcriptionally controlled. The results of heterologous gene fusions between the actin gene promoter and *CIT2* and between the *CIT2* promoter and the *E. coli lacZ* gene show that the elevated expression of *CIT2* in a [*rho*^{0}] petite is controlled transcriptionally by 5′-flanking *CIT2* DNA sequences. Partelidis and Mason (25) have described a similar dependence on upstream sequences for elevated expression in a [*rho*^{0}] of *MRP13*, a nuclear gene encoding a mitochondrial ribosomal protein. While further work will be required to define the *cis*-acting sequences in those genes responsible for their increased expression in respiratory-deficient cells, it is interesting that both genes contain a version of a mitochondrial DNA RNA polymerase promoter element (MPE) (at −134 for *CIT2* and at −281 for *MRP13* [25]) in their 5′-flanking DNA. MPEs have been found in a number of nuclear genes in yeast cells, and some can function in vitro as a transcriptional start site for the nuclear-encoded mitochondrial RNA polymerase (18). Furthermore, there is some indication that when present in certain contexts upstream of a gene, MPEs can effect an elevated expression of that gene in respiratory-deficient cells (9a, 18).

There is little information on the mechanism of this path of communication from mitochondria to the nucleus. However, our observations on *CIT2* expression may offer some interesting clues as to how nuclear gene expression could be affected by alteration of mitochondrial function. That the dependence of *CIT2* expression on mitochondrial function is complex is underscored by the observation that *CIT2* expression can also be increased in [*rho*$^+$] cells by the addition of the respiratory chain inhibitor antimycin A and by a disruption of the *CIT1* gene. These effects appear to be roughly additive: each alone gives a significant but only partial induction of *CIT2* mRNA relative to the level in the [*rho*^{0}] petite. These data suggest the presence of at least two *cis*-acting elements responsive to different alterations in mitochondrial function within the 605-bp 5′-flanking DNA of *CIT2*. The most straightforward interpretation of the available data is that inhibition of the TCA cycle and oxidative phosphorylation, neither of which functions in petites, could provide independent signals that would be relayed to the *CIT2* gene, affecting its transcription. The molecular characteristics of the signals, and whether these effects apply to other genes whose expression is modulated by the mitochondrial state, remain to be established.

There are many examples of nuclear-encoded mitochondrial proteins that are affected by different physiological and metabolic factors, such as heme, oxygen, and carbon source (see reference 9 for a recent review). In one of the best-studied examples, expression of the *CIT1* gene is controlled through two upstream activation sequence (UAS) elements, one (UAS1) responsive largely to heme and the other (UAS2) responsive largely to carbon source (10, 11). These UAS elements are targets for *trans*-acting factors, HAP 1 to 4 (9, 22, 26), that also act as transcriptional regulators for several other nuclear genes (36, 39). Our results with *CIT2*, indicating that the petite-dependent elevated expression can be separated into at least two metabolically related components, suggest that expression of this gene may be regulated by different 5′-flanking domains.

Metabolic considerations of *CIT2* regulation. In light of the available data, it is of interest to consider the possible metabolic interplay between two isoforms of citrate synthase, each sequestered within separate organelles. In cells growing aerobically on all substrates except acetate or those that yield C_2 units only (such as fatty acids), the TCA cycle (which uses CS 1) can supply both energy and intermediates for growth. The glyoxylate cycle using CS 2 is needed only for growth on acetate or acetogenic substances. Although there are no available data for yeast cells that assess the relative contribution of these two cycles growth in various media, we have reported that CS2$^-$ cells grow the same as wild-type cells on all media tested (15). We have suggested further that citrate generated in mitochondria can serve as a source of citrate to operate the glyoxylate cycle (15). Similarly, under certain conditions, citrate generated from the glyoxylate cycle may be available, though inefficiently so, to mitochondria to allow the TCA cycle to function in the absence of CS 1 activity (14). The data presented here provide additional support for such a functional link between the citrate synthase isozymes. Disruptions of *CIT1* and *CIT2*, singly or in combination, have no major effect on growth rate of the [*rho*$^+$] or [*rho*^{0}] cells growing in rich raffinose medium. However, in a *CIT1 CIT2* double disruption, growth yield in the [*rho*$^+$] cells was reduced to nearly 50% that of the wild-type [*rho*$^+$] cells, but the double

disruption had little effect in [*rho*^{0}] cells. This latter result is reasonable, since neither CS 1 nor CS 2 should play any significant metabolic role in cells lacking both respiration and a functional TCA cycle, as in [*rho*^{0}] petite cells. Thus, the increase in CS 2 mRNA in respiratory-deficient cells or in cells without CS 1 activity may reflect an attempt to find a source of synthesis of needed intermediates for cell growth. The identities of the signals that effect this increase are under investigation.

ACKNOWLEDGMENTS

We thank L. Guarente and M. Rosencrantz for PSY yeast strains.

This work was supported by grants GM22525 from the NIH and I-642 from the Robert A. Welch Foundation to R.A.B. and by grants from the Veterans Administration, DK11313 from the NIH, and DCB 8821560 from the NSF to P.A.S.

REFERENCES

1. **Attardi, G., and G. Schatz.** 1988. Biogenesis of mitochondria. Annu. Rev. Cell Biol. **4**:289–333.
2. **Bradford, M. M.** 1976. A rapid and sensitive method for the quantitation of microgram quantities of protein utilizing the principle of protein-dye binding. Anal. Biochem. **72**:248–254.
3. **Butow, R. A., R. Docherty, and V. S. Parikh.** 1988. A path from mitochondria to the yeast nucleus. Philos. Trans. R. Soc. London **319**:127–133.
4. **Dang, H., G. Franklin, K. Darlak, A. F. Spatola, and S. R. Ellis.** 1990. Discoordinate expression of the yeast mitochondrial ribosomal protein MRP1. J. Biol. Chem. **265**:7449–7454.
5. **Daum, G., P. C. Bohni, and G. Schatz.** 1982. Import of proteins into mitochondria. Cytochrome b2 and cytochrome c peroxidase are located in the intramembrane space of yeast mitochondria. J. Biol. Chem. **257**:13028–13033.
6. **Douglas, M. G., B. L. Geller, and S. D. Emr.** 1984. Intracellular targeting and import of an F1-ATPase beta-subunit-beta galactosidase hybrid protein into yeast mitochondria. Proc. Natl. Acad. Sci. USA **81**:3983–3987.
7. **Elion, E. A., and J. R. Warner.** 1984. The major promoter element of rRNA transcription in yeast lies 2 kb upstream. Cell **39**:663–673.
8. **Fearon, K., and T. L. Mason.** 1988. Structure and regulation of a nuclear gene in *Saccharomyces cerevisiae* that specifies MRP7, a protein of the large subunit of the mitochondrial ribosome. Mol. Cell. Biol. **8**:3636–3646.
9. **Forsburg, S. L., and L. Guarente.** 1989. Communication between mitochondria and the nucleus in regulation of cytochrome genes in the yeast *Saccharomyces cerevisiae*. Annu. Rev. Cell Biol. **5**:153–180.

9a. **Grossfeld, P.** Unpublished data.

10. **Guarente, L., B. Lalonde, P. Gifford, and E. Alani.** 1984. Distinctly regulated tandem upstream activation sites mediate catabolite expression of the *CYC1* gene of *S. cerevisiae*. Cell **36**:503–511.
11. **Guarente, L., and T. Mason.** 1983. Heme regulates transcription of the *CYC1* gene in *S. cerevisiae* via an upstream activation site. Cell **32**:1279–1286.
12. **Ito, H., Y. Fukuda, K. Murata, and A. Kimura.** 1983. Transformation of intact yeast cells treated with alkali cations. J. Bacteriol. **153**:163–168.
13. **Kim, K. S., M. S. Rosenkrantz, and L. Guarente.** 1986. *Saccharomyces cerevisiae* contains two functional citrate synthase genes. Mol. Cell. Biol. **6**:1936–1942.
14. **Kispal, G., C. T. Evans, C. Malloy, and P. A. Srere.** 1989. Metabolic studies on citrate synthase mutants of yeast: a change in phenotype following transformation with an inactive enzyme. J. Biol. Chem. **264**:11204–11210.
15. **Kispal, G., M. Rosenkrantz, L. Guarente, and P. A. Srere.** 1988. Metabolic changes in *Saccharomyces cerevisiae* strains lacking citrate synthase. J. Biol. Chem. **263**:11145–11149.
16. **Kornberg, H. L.** 1966. The role and control of the glyoxylate cycle in *E. coli*. Biochem. J. **99**:1–11.
17. **Lewin, A. S., V. Hines, and G. M. Small.** 1990. Citrate synthase encoded by the *CIT2* gene of *Saccharomyces cerevisiae* is peroxisomal. Mol. Cell. Biol. **10**:1399–1405.
18. **Marczynski, G. T., P. W. Schultz, and J. A. Jaehning.** 1989. Use of yeast nuclear DNA sequences to define the mitochondrial RNA polymerase promoter in vitro. Mol. Cell. Biol. **9**:3193–3202.
19. **Melton, D. A., P. A. Krieg, M. R. Rebagliati, T. Maniatis, K. Zinn, and M. R. Green.** 1984. Efficient *in vitro* synthesis of biologically active RNA and RNA hybridization probes form plasmids containing a bacteriophage SP6 promoter. Nucleic Acids Res. **12**:7035–7056.
20. **Ng, R., and J. Abelson.** 1980. Isolation and sequence of the gene for actin in *Saccharomyces cerevisiae*. Proc. Natl. Acad. Sci. USA **77**:3912–3916.
21. **Nunez de Castro, T., J. M. Arias de Saavedra, A. Machado, and F. Mayor.** 1976. Regulation of the level of yeast citrate synthase by oxygen availability. Mol. Cell. Biochem. **12**:161–169.
22. **Olesen, J. T., S. Hahn, and L. Guarente.** 1987. Yeast HAP2 and HAP3 activators both bind to the *CYC1* upstream activation site UAS2 in an interdependent manner. Cell **51**:953–961.
23. **Parikh, V. S., H. Conrad-Webb, R. Docherty, and R. A. Butow.** 1989. Interaction between the yeast mitochondrial and nuclear genomes influences the abundance of novel transcripts derived from the spacer region of the nuclear ribosomal DNA repeat. Mol. Cell. Biol. **9**:1897–1907.
24. **Parikh, V. S., M. M. Morgan, R. Scott, L. S. Clements, and R. A. Butow.** 1987. The mitochondrial genotype can influence nuclear gene expression in yeast. Science **235**:576–580.
25. **Partelidis, J. A., and T. L. Mason.** 1988. Structure and regulation of a nuclear gene in *Saccharomyces cerevisiae* that specified MRP13, a protein of the small subunit of the mitochondrial ribosome. Mol. Cell. Biol. **8**:3647–3660.
26. **Pfeifer, K., T. Prezant, and L. Guarente.** 1987. Yeast HAP1 activator binds to two upstream sites of different sequences. Cell **49**:291–301.
27. **Rickey, T. M., and A. L. Lewin.** 1986. Extramitochondrial citrate synthase activity in bakers' yeast. Mol. Cell. Biol. **6**:488–493.
28. **Rose, M., and D. Botstein.** 1983. Construction and use of gene fusions of LacZ (β-galactosidase) which are expressed in yeast. Methods Enzymol. **101**:167–180.
29. **Rosenkrantz, M., T. Alam, K. Kim, B. J. Clark, P. A. Srere, and L. P. Guarente.** 1986. Mitochondrial and nonmitochondrial citrate synthases in *Saccharomyces cerevisiae* are encoded by distinct homologous genes. Mol. Cell. Biol. **6**:4509–4515.
30. **Sanger, F., S. Nicklen, and A. R. Coulson.** 1977. DNA sequencing with chain-terminating inhibitors. Proc. Natl. Acad. Sci. USA **74**:5463–5467.
31. **Sikorski, R. S., and P. Hieter.** 1989. A system of shuttle vectors and yeast host strains designed for efficient manipulation of DNA in *Saccharomyces cerevisiae*. Genetics **122**:19–27.
32. **Simon, E. J., and D. J. Shemin.** 1953. The preparation of S-succinyl coenzyme A. J. Am. Chem. Soc. **75**:2520–2524.
33. **Srere, P. A., H. Brazil, and L. Gonen.** 1963. The citrate condensing enzyme of pigeon breast muscle and moth flight muscle. Acta Chem. Scand. **72**:S129–S134.
34. **Suissa, M., K. Suda, and G. Schatz.** 1984. Isolation of the nuclear yeast genes for citrate synthase and fifteen other yeast mitochondrial proteins by a new screening method. EMBO J. **3**:1773–1781.
35. **Szekely, E., and D. L. Montgomery.** 1984. Glucose represses transcription of *Saccharomyces cerevisiae* nuclear genes that encode mitochondrial components. Mol. Cell. Biol. **4**:939–946.
36. **Trawick, J. D., R. M. Wright, and R. O. Poyton.** 1989. Transcription of yeast COX6, the gene for cytochrome c oxidase subunit VI, is dependent on heme and on the HAP2 gene. J. Biol. Chem. **264**:7005–7008.
37. **Tzagoloff, A., and A. M. Myers.** 1986. Genetics of mitochondrial biogenesis. Annu. Rev. Biochem. **55**:249–285.
38. **Wang, S.-S., and M. C. Brandriss.** 1987. Proline utilization in *Saccharomyces cerevisiae*: sequence, regulation, and mito-

chondrial localization of the *PUT1* gene product. Mol. Cell. Biol. 7:4431–4440.

39. **Winkler, H., G. Adam, E. Mattes, M. Schanz, A. Hartig, and H. Ruis.** 1988. Co-ordinate control of synthesis of mitochondrial and nonmitochondrial hemoproteins: a binding site for the HAP1 (*CYP1*) protein in the UAS region of the yeast catalase T gene (*CTT1*). EMBO J. 7:1799–1804.
40. **Zhu, H., H. Conrad-Webb, X. S. Liao, P. S. Perlman, and R. A. Butow.** 1989. Functional expression of a yeast mitochondrial intron-encoded protein requires RNA processing at a conserved dodedamer sequence at the 3′ end of the gene. Mol. Gen. Genet. 9:1507–1512.